

Progress on electrocaloric multilayer ceramic capacitor development

Sakyo Hirose,^{1,a)} Tomoyasu Usui,¹ Sam Crossley,² Bhasi Nair,² Akira Ando,¹ Xavier Moya² and Neil D. Mathur²

¹*Murata Manufacturing Co., Ltd., 1-10-1, Higashikotari, Nagaokakyo, Kyoto 617-8555, Japan*

²*Department of Materials Science & Metallurgy, University of Cambridge, Cambridge, CB3 0FS, UK*

A multilayer capacitor comprising 19 layers of 38 μm -thick $0.9\text{Pb}(\text{Mg}_{1/3}\text{Nb}_{2/3})\text{O}_3$ – 0.1PbTiO_3 has elsewhere been shown to display electrocaloric temperature changes of 2.2 K due to field changes of $24 \text{ V } \mu\text{m}^{-1}$, near $\sim 100^\circ\text{C}$. Here we demonstrate temperature changes of 1.2 K in an equivalent device with 2.6 times the thermal mass, i.e. 49 layers that could tolerate $10.3 \text{ V } \mu\text{m}^{-1}$. Breakdown was compromised by the increased number of layers, and occurred at $10.5 \text{ V } \mu\text{m}^{-1}$ near the edge of a near-surface inner electrode. Further optimization is required to improve the breakdown strength of large electrocaloric multilayer capacitors for cooling applications.

^{a)} Author to whom correspondence should be addressed. Electronic mail: h_sakyo@murata.com.

Ever since the 1920 discovery of ferroelectricity in Rochelle salt, ferroelectric materials have attracted significant attention on account of their unique electrical properties, e.g. spontaneous polarization, switchable polarization, large dielectric permittivity, and large piezoelectric effects.¹ Since the 1950s, these properties have enabled the realization of many indispensable electronic devices, such as sensors, actuators, filters, thermistors, capacitors, and memory devices.²⁻⁴

The electrocaloric (EC) effect, of interest here, describes reversible thermal changes that arise in materials from changes of electric field E . It has been observed to peak near the Curie temperature T_C in various ferroelectric materials, where phase transitions may be electrically driven and undriven. EC effects in bulk samples are traditionally considered to be small. However, in the 2000s, larger EC effects were reported for thin films of ceramics and polymers.^{5,6} Mischenko *et al.* reported a large adiabatic temperature change of $|\Delta T| = 12$ K in 350 nm-thick films of $\text{PbZr}_{0.95}\text{Ti}_{0.05}\text{O}_3$ near $T_C = 222$ °C,⁵ whereas Neese *et al.* reported $|\Delta T| = 12$ K in micron-thick films of the ferroelectric poly(vinylidene fluoride-trifluoroethylene) copolymer near 80 °C.⁶ These reports stimulated research on EC materials, for solid-state cooling applications with low-energy consumption, no noise, and small device size.⁷⁻¹² This research is now particularly timely given that new cooling technologies are becoming increasingly important in electronics and applications such as refrigerators and air conditioners.

The key advantage of thin films is that they possess a large breakdown strength compared with bulk ceramics, where EC effects are smaller as they cannot be driven so hard.^{13,14} Moreover, the key disadvantage of thin films (low thermal mass) can be overcome by combining many films to form a multilayer capacitor (MLC).⁹⁻¹² As explained in ref. 9, this represents an attractive geometry for cooling applications because there is little unwanted thermal mass, and good thermally conducting pathways via the inner electrodes.

We have recently studied EC effects in films of $0.9\text{Pb}(\text{Mg}_{1/3}\text{Nb}_{2/3})\text{O}_3$ - 0.1PbTiO_3 [90PMN-10PT] that were fabricated using conventional MLC technology to yield single layers on 0.5 mm-thick substrates,¹⁵ and 19 layers with no substrate.¹⁶ For the single-layer devices, adiabaticity was severely

compromised by the substrate, but scanning thermal microscopy was able to record a non-adiabatic temperature change of $|\Delta T^*| \sim 0.23$ K for both a thinner film driven with a larger field, and a thicker film driven with a smaller field ($31 \text{ V } \mu\text{m}^{-1}$ across $13 \text{ } \mu\text{m}$, and $11 \text{ V } \mu\text{m}^{-1}$ across $38 \text{ } \mu\text{m}$, near room temperature). For the 19-layer MLC with no substrate and a total active area of 5.4 cm^2 , we used a thermocouple to record an order of magnitude larger value of $|\Delta T| \sim 2.2$ K for similar changes of field ($24 \text{ V } \mu\text{m}^{-1}$ across $38 \text{ } \mu\text{m}$, near $105 \text{ }^\circ\text{C}$). This temperature change is understood to be adiabatic given that it corresponds well to the values we present later for our 49-layer device at lower fields. However, it remains desirable to increase the number and area of active layers in order to pump more heat.

Here we report on the dielectric, ferroelectric, and EC properties of a large MLC with external dimensions $10 \text{ mm} \times 7 \text{ mm} \times 2.4 \text{ mm}$. Fabrication and characterization methods were analogous to those used for the 19-layer MLC,¹⁶ and are described in supplementary material along with the corresponding details for a $300 \text{ } \mu\text{m}$ -thick plate ceramic with which we make comparison.¹⁷ Our 49 layers of $38 \text{ } \mu\text{m}$ -thick 90PMN-10PT presented a total active area of 14 cm^2 to pairs of platinum inner electrodes connected to silver outer electrodes. 90PMN-10PT was chosen because it displays good EC properties in a wide range of temperatures, near room temperature.^{15-16,18} Electrically driven jumps of ΔT that arise over a short time t in direct measurements of temperature change $\Delta T_\#(t)$ are assumed to be adiabatic, and to represent the active regions alone such that we neglect the thermal mass of the thermocouple used for measurement, the electrodes, a $38 \text{ } \mu\text{m}$ -thick surface layer of inactive ceramic, and inactive ceramic regions that lay far from the thermocouple. We will finish by discussing various technical issues that surround the development of MLC prototypes for EC applications.

A photograph of the device alongside a smaller conventional MLC based on BaTiO_3 is shown in Fig. 1(a). A cross-sectional image obtained using a laser microscope (VK-9510, Keyence) is shown in Fig. 1(b), with a device schematic as inset. The temperature dependence of the dielectric response [Fig. 1(c)] was restricted to the frequency range $1\text{--}10 \text{ kHz}$ due to a self-resonance around 200 kHz . The maxima in permittivity occurred at $T_m \sim 50 \text{ }^\circ\text{C}$ as expected,^{16,19} and showed the well-known

frequency dependence associated with relaxors. Above 100 °C, the dielectric loss $\tan \delta < 3\%$, even at 1 kHz, consistent with a large electrical resistance that is important in order to avoid Joule heating while waiting for heat to flow out of the charged device. Ferroelectric polarization loops were measured from 25 to 180 °C [Fig. 1(d)]. The room-temperature spontaneous polarization is $\sim 20 \mu\text{C cm}^{-2}$ as expected,^{16,19} and ferroelectricity persists up to ~ 100 °C.

Fig. 2(a) shows EC temperature change $\Delta T_{\#}(t)$ arising from field changes of $7.9 \text{ V } \mu\text{m}^{-1}$, at various starting temperatures. Field application (arrowed black) led to an increase of MLC temperature due to EC heating ($\Delta T > 0$). Heat subsequently leaked out of the MLC over ~ 60 s, which is similar to the value obtained for commercially available MLCs showing smaller EC effects.⁹ After this wait time, the starting temperature was approximately recovered with the field still applied, consistent with negligible Joule heating from a leakage current that remained very small due to high electrical resistivity ($< 20 \mu\text{A}$, even at 140 °C). Negligible Joule heating also ensured that EC cooling on field removal ($\Delta T < 0$, arrowed red) was almost as large as the EC heating on field application. Our largest value of $|\Delta T| = 0.82 \text{ K}$ was obtained at 100 °C for a field change of $7.9 \text{ V } \mu\text{m}^{-1}$. The resulting value of EC strength $|\Delta T|/|\Delta E| = 0.1 \text{ K V}^{-1} \mu\text{m}$ matches the value obtained for our 19-layer device,¹⁶ whose adiabaticity is thus confirmed to be good.

When varying the starting temperature and $|\Delta E|$ [Fig. 2(b)], we see that $|\Delta T|$ remains very similar for field application and removal; and that there is a peak in $|\Delta T|$ versus starting temperature. Moreover, on decreasing $|\Delta E|$ from $7.9 \text{ V } \mu\text{m}^{-1}$ to $2.6 \text{ V } \mu\text{m}^{-1}$, our optimal operating temperature of $T_0 \sim 100$ °C was reduced to around 50-80 °C, confirming that low-field operation is optimised near $T_m \sim 50$ °C. This variation of T_0 with $|\Delta E|$ has been reported previously.¹⁸ It may be attributed to the field-induced alignment and growth of polar nanoregions, and should be taken into account when determining the operating temperature of EC cooling devices based on relaxor ferroelectrics.

Next, we explored the effect on $\Delta T_{\#}(t)$ of increasing $|\Delta E|$ above $7.9 \text{ V } \mu\text{m}^{-1}$, at a starting temperature of 100 °C [Fig. 3(a)]. Three apply/remove cycles were performed for $10.3 \text{ V } \mu\text{m}^{-1}$, and breakdown occurred at the start of the second cycle with $10.5 \text{ V } \mu\text{m}^{-1}$. Although the initial application

of this largest field produced the largest increase in MLC temperature, we did not observe a concomitantly large EC cooling on field removal, probably due to the onset of breakdown. Therefore our largest reversible value of $|\Delta T| = 1.2$ K was obtained for the field change of $10.3 \text{ V } \mu\text{m}^{-1}$. We anticipate that this value would have been larger at higher temperature, given the increase of peak temperature with increasing field [Fig. 2(b)], but this could not be explored in the destroyed sample. Our 49-layer MLC here, and the 19-layer MLC reported previously,¹⁶ show a similar variation of $|\Delta T|$ with $|\Delta E|$ [Fig. 3(b)], but the larger device experienced failure at a lower field, consistent with the higher probability of breakdown in samples of larger area.

The similar values of $|\Delta T|/|\Delta E|$ for the two MLCs are also similar with respect to our $300 \text{ } \mu\text{m}$ -thick plate ceramic, which supported the smaller field of $3.3 \text{ V } \mu\text{m}^{-1}$ [this comparison is made in the inset of Fig. 3(b) and Table 1, with an example of raw data for the plate ceramic in supplementary material (Sup. Fig. 1)¹⁷]. By contrast, bulk samples that were thinned^{18,20} to increase breakdown field show values of $|\Delta T|/|\Delta E|$ that are roughly twice as large (Table 1), possibly due to variations in fabrication, grain size, measurement and inactive volume. However, if one is prepared to apply larger fields, then MLCs offer similar values of $|\Delta T|$ with 90PMN-10PT layers that are collectively much thicker than the thinned bulk samples. Moreover, increasing the number of layers does not necessarily compromise the speed of heat flow in general, as the inner electrodes possess good thermal conductivity.

In order to understand the origin of the breakdown observed in our MLC, we conducted a failure analysis. A plan-view photograph [Fig. 3(c)] revealed that the breakdown spot lay near inner electrode edges. A cross-section obtained by polishing as little as necessary [Fig. 3(d)] revealed damage in two near-surface ceramic layers, whose intervening platinum electrode had melted, evidencing extremely high temperatures due to high current densities.

In capacitors and piezoelectric actuators, there are several kinds of degradation phenomena²¹⁻²⁵ that are promoted by constant field at high-temperatures, large ac or dc fields, and high humidity. The resulting degradation is associated with the migration of defects such as oxygen vacancies, electrochemical reactions, heating, cracking/delamination from piezoelectricity/electrostriction, and

structural flaws such as delamination, pores, and misaligned electrodes. Breakdown observed near electrode edges is considered to be the result of field concentration and internal stress that arise from the field-driven strain in the active ferroelectric layers. Given that degradation is statistically more likely with larger electrodes and overly thin active layers, samples with a large total area and thin active layers typically possess lower breakdown fields. Therefore it is challenging to achieve high-field operation in MLCs with a large number of thin active layers, but MLC fabrication and device structure have not yet been optimized at the current stage of development.

The fields required for EC effects are much larger than those experienced by other dielectric and piezoelectric devices. Reliable operation at over $10 \text{ V } \mu\text{m}^{-1}$ will be challenging, but we are encouraged by the fact that our 19-layer MLC worked reliably at $24 \text{ V } \mu\text{m}^{-1}$.¹⁶ Current results are too preliminary to merit studies of reliability, but in future MLCs it will be important to achieve the sustained and repeated use of large fields for practical EC applications.

In summary, we have studied an MLC based on 49 layers of 90PMN-10PT. At a starting temperature of 100°C , we observed reversible adiabatic temperature changes of 1.2 K for field changes of $10.3 \text{ V } \mu\text{m}^{-1}$, and a wide temperature range of operation (e.g. $\sim 60\text{--}120^\circ\text{C}$) is expected based on our data at lower fields. The active thermal mass is increased by a factor of 2.6 with respect to a similar 19-layer MLC¹⁶ that shows the same EC strength $|\Delta T|/|\Delta E| = 0.1 \text{ K V}^{-1} \mu\text{m}$. The large number of active layers compromises breakdown strength because the total area of the inner electrodes is large and because cumulative internal stresses are increased. It may be possible to increase the breakdown field to the $20 \text{ V } \mu\text{m}^{-1}$ that we achieved in our 19-layer MLC¹⁶ by optimizing fabrication and device structure. Device structure may also be simultaneously optimized via finite element analysis in order to maximise heat flow via the inner electrodes.²⁶ More generally, further investigations are required to demonstrate new EC materials for use in practical cooling applications based on MLCs.

Acknowledgements

X.M. is grateful for support from the Royal Society. B.N. is grateful for the support from Gates Cambridge and the Winton Programme for the Physics of Sustainability.

References

1. E. T. Jaynes, *Ferroelectricity* (Princeton University Press, 1953).
2. W. Heywang and H. Thomann, *An. Rev. Mater. Sci.* **14**, 27 (1984).
3. H. Kishi, Y. Mizuno, and H. Chazono, *Jpn. J. Appl. Phys.* **42**, 1 (2003).
4. J. F. Scott, A. Paz, and A. Carlos, *Science* **246**, 1400 (1989).
5. A. S. Mischenko, Q. Zhang, J. F. Scott, R. W. Whatmore, and N. D. Mathur, *Science* **311**, 1270 (2006).
6. B. Neese, B. Chu, S.-G. Lu, Y. Wang, E. Furman, and Q. M. Zhang, *Science* **321**, 821 (2008).
7. X. S. Qian, H. J. Ye, Y. T. Zhang, H. Gu, X. Li, C. A. Randall, and Q. M. Zhang, *Adv. Funct. Mater.* **24**, 1300 (2014).
8. B. Peng, H. Fan, and Q. Zhang, *Adv. Func. Mater.* **23**, 2987 (2013).
9. S. Kar-Narayan and N. D. Mathur, *Appl. Phys. Lett.* **95**, 242903 (2009).
10. R. I. Epstein and K. J. Malloy, *J. Appl. Phys.* **106**, 064509 (2009).
11. Y. Bai, G.-P. Zheng, K. Ding, L. Qiao, S.-Q. Shi, and D. Guo, *J. Appl. Phys.* **110**, 094103 (2011).
12. D. Guo, J. Gao, Y.-J. Yu, S. Santhanam, A. Slippey, G. K. Fedder, A. J. H. McGaughey, and S.-C. Yao, *Int. J. Heat. Mass. Trans.* **72**, 559 (2014).
13. X. Moya, S. Kar-Narayan, and N. D. Mathur, *Nat. Mater.* **13**, 439 (2014).
14. S. Crossley, N. D. Mathur, and X. Moya, *AIP Adv.* **5**, 067153 (2015).

15. S. Crossley, T. Usui, B. Nari, S. Kar-Narayan, X. Moya, S. Hirose, A. Ando, and N. D. Mathur, Appl. Phys. Lett. **108**, 032902 (2016) .
16. T. Usui, S. Hirose, S. Crossley, B. Nari, S. Kar-Narayan, X. Moya, and N. D. Mathur, to be submitted.
17. See supplementary material for details of sample fabrication, measurement methods, and electrocaloric data for a plate ceramic of thickness 300 μm .
18. J. Peräntie, H. N. Taylor, J. Hagberg, H. Jantunen, and Z.-G. Ye, J. Appl. Phys. **114**, 174105 (2013).
19. J. Hagberg, A. Uusimäki, and H. Jantunen, Appl. Phys. Lett. **92**, 132909 (2008).
20. M. Vrabelj, H. Uršič, Zdravko Kutnjak, B. Rožič, S. Drnovšek, A. Benčan, V. Bobnar, L. Fulanović and B. Malič, J. Eur. Ceram. Soc. **36**, 75 (2016).
21. R. Waser, T. Baiatu, and K.-H. Hardtl, J. Am. Ceram. Soc. **73**, 1645 (1990).
22. N. Shankar and A. P. Ritter, J. Am. Ceram. Soc. **72**, 2246 (1989).
23. S. R. Winzer, N. Shankar, and A. P. Ritter, J. Am. Ceram. Soc. **72**, 2246 (1989).
24. J. Glaum and M. Hoffman, J. Am. Ceram. Soc. **97**, 665 (2014).
25. P. Pertsch, S. Richter, D. Kopsch, N. Kramer, J. Pogodzick, and E. Henning, in *Actuator 2006 Conference Proceedings*, pp. 14–16 (2006).
26. S. Crossley, J. R. McGinnigle, S. Kar-Narayan and N. D. Mathur, Appl. Phys. Lett. **104**, 082909 (2014).

Sample type	Number of layers	Layer thickness (μm)	T_0 ($^{\circ}\text{C}$)	$ \Delta T $ (K)	$ \Delta E $ ($\text{V } \mu\text{m}^{-1}$)	$ \Delta T / \Delta E $ ($\text{K V}^{-1} \mu\text{m}$)	Ref.
MLC	49	38	100	1.2 0.3	10.3 3.2	0.12 0.11	This work
MLC	19	38	100	2.2 0.3	24 3.2	0.10 0.10	16
Plate ceramic	1	300	100	0.4	3.3	0.12	This work
Thinned bulk	1	120	90	1.2	5	0.24	18
Thinned bulk	1	80	127	3.5	16	0.22	20

Table 1. Comparison of EC properties for different types of 90PMN-10PT sample, measured with a thermocouple. Optimal operating temperature is denoted T_0 . EC temperature change $|\Delta T|$ is considered to be adiabatic and to represent the active regions alone.

Figures

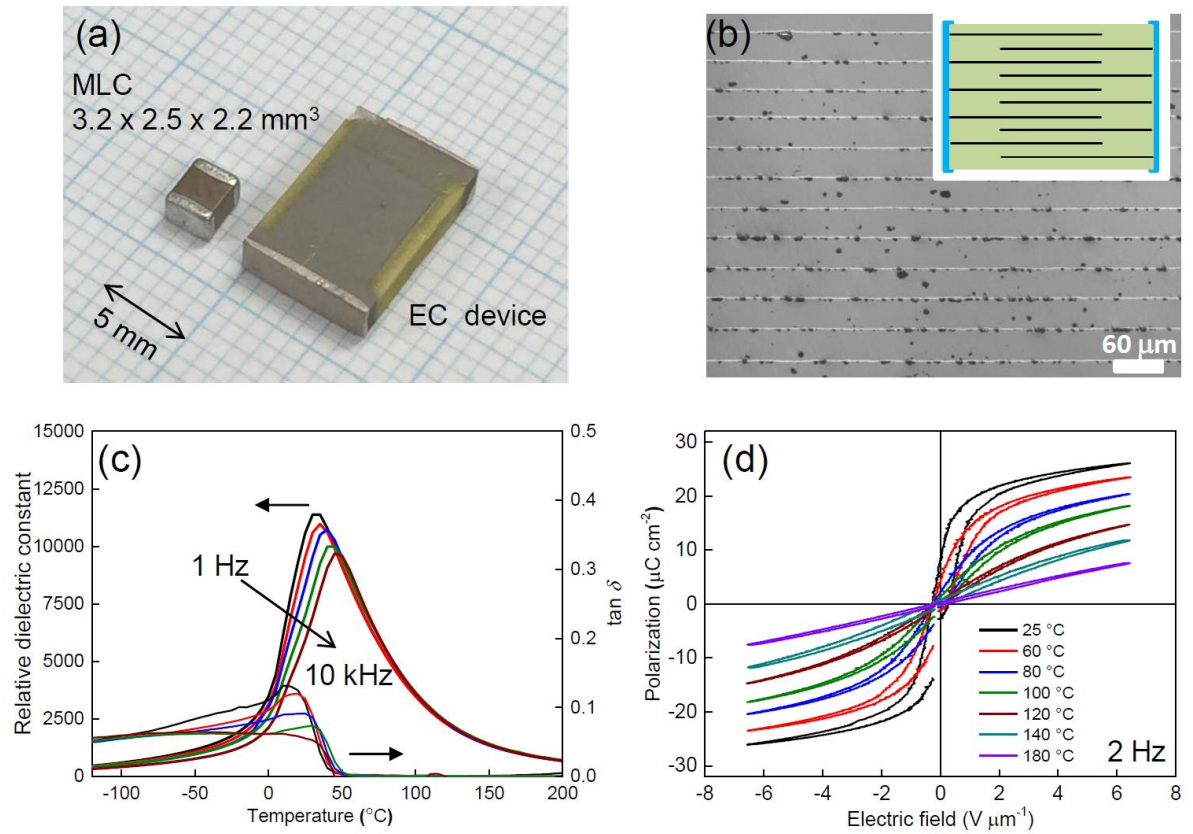


Figure 1. Characterization of prototype EC device with 49 layers. (a) Photograph of EC device with 3225-size MLC for comparison. (b) Cross-sectional optical microscopy image from within the EC device, whose simplified schematic is shown in the inset. In reality, there are 49 layers of 90PMN-10PT (green) between 50 interdigitated Pt inner electrodes (black) that are addressed via two Ag outer electrodes (blue). (c) Relative dielectric constant and loss $\tan \delta$ versus temperature at various frequencies. (d) Electrical polarization versus field, at various temperatures including room temperature. Data in (c,d) measured on heating.

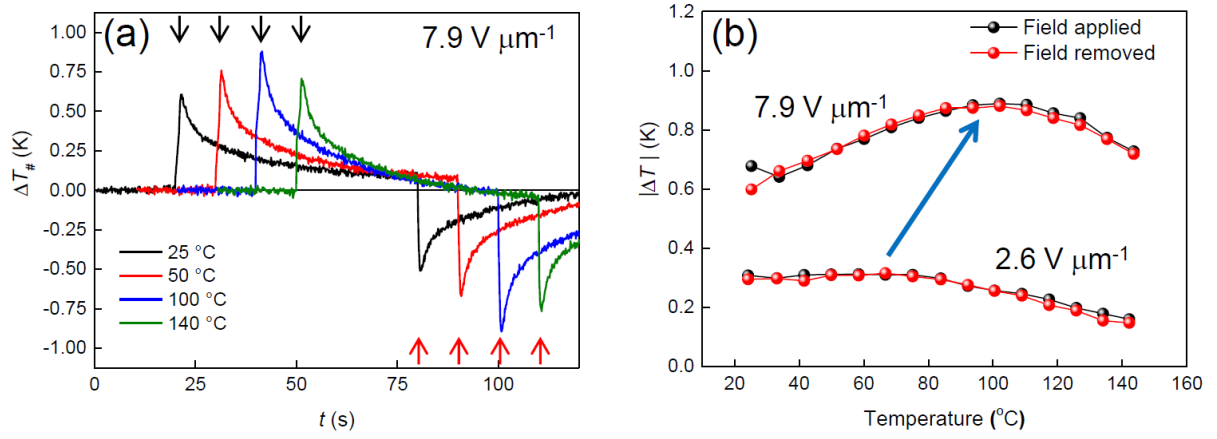


Figure 2. Temperature and field dependence of EC effects in 49-layer MLC. (a) Measured temperature change $\Delta T_{\#}$ versus time t due to the application and removal of $7.9 \text{ V } \mu\text{m}^{-1}$, at various temperatures. Black and red arrows denote field application and removal, respectively. (b) Adiabatic temperature change $|\Delta T|$ versus starting temperature, for two values of field change. Blue arrow denotes shift of maximum temperature change. Data measured on heating.

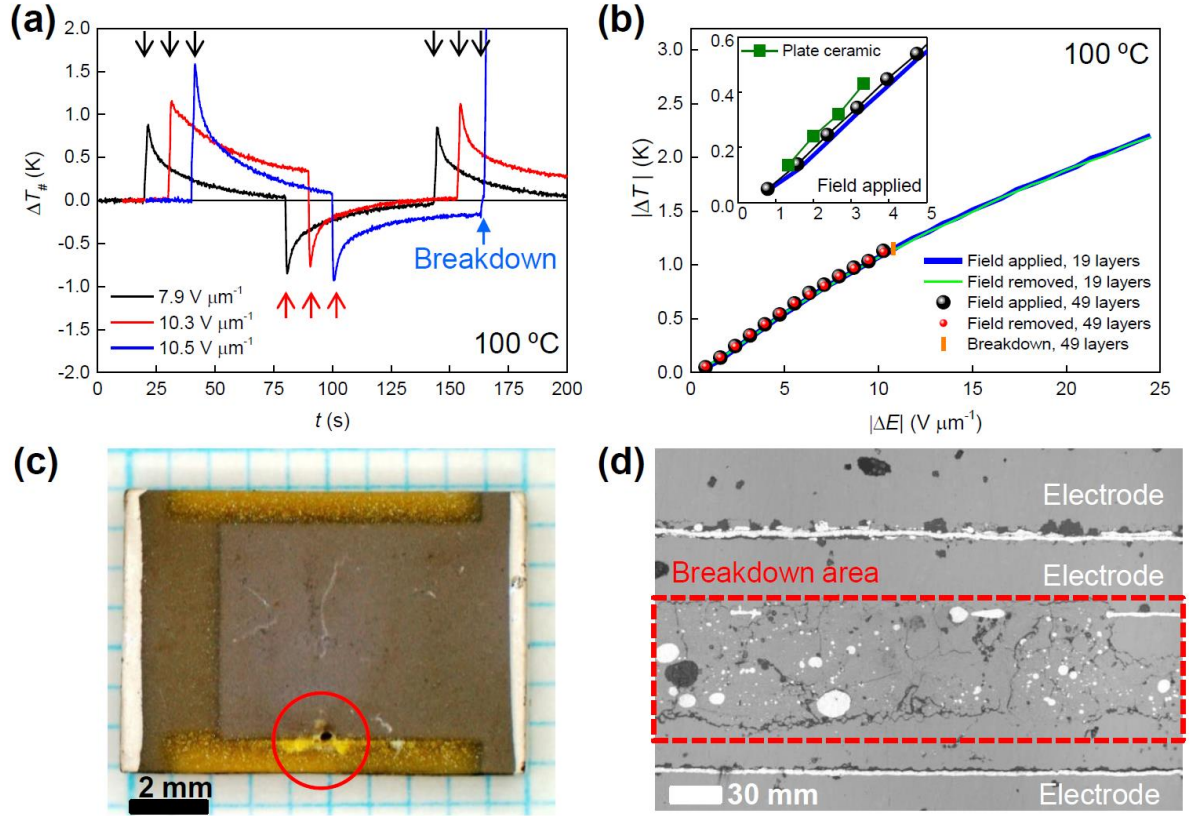


Figure 3. Field dependence of EC effects and breakdown in 49-layer MLC at 100 °C. (a) Measured temperature change $\Delta T_{\#}$ versus time t due to various changes of field. Data for 7.9 $\text{V } \mu\text{m}^{-1}$ are similar to data shown in Fig. 2(a). (b) Adiabatic temperature change ΔT versus field change ΔE , for MLCs with 19 and 49 active layers. The inset plotted on the same axes shows the low-field applied data for these samples and also the plate ceramic. (c) Photograph of the EC device after breakdown has occurred in the dark region circled red. (d) Cross-sectional optical microscopy image obtained after breakdown has occurred in the region surrounded by the dashed red line. One can observe a melted electrode, and degradation in active layers 2 and 3.

Supplementary information
for
Progress on electrocaloric multilayer ceramic capacitor development

Sakyo Hirose,^{1,a)} Tomoyasu Usui,¹ Sam Crossley,² Bhasi Nair,² Akira Ando,¹ Xavier Moya² and Neil D. Mathur²

¹*Murata Manufacturing Co., Ltd., 1-10-1, Higashikotari, Nagaokakyo, Kyoto 617-8555, Japan*

²*Department of Materials Science & Metallurgy, University of Cambridge, Cambridge, CB3 0FS, UK*

This file comprises a description of sample fabrication, measurement methods, and electrocaloric data for a plate ceramic of thickness 300 μm .

MLC sample fabrication was based on the MLC processing method that we now describe. Initially, we prepared a powder of MgNb_2O_6 from high purity powders of MgCO_3 and Nb_2O_5 by first ball milling with partially stabilized zirconia (PSZ) balls of diameter of 2 mm for 24 hours, and then drying, pulverizing, and calcining at 1100 °C for 12 hours. We subsequently prepared a powder of $0.9\text{Pb}(\text{Mg}_{1/3}\text{Nb}_{2/3})\text{O}_3$ - 0.1PbTiO_3 from powders of MgNb_2O_6 , Pb_3O_4 (Pb 2 mol% excess) and TiO_2 by first ball milling for 24 hours, and then drying, pulverizing, and calcining again at 900 °C for 4 hours. This powder was ball-milled in an organic solvent and binder to produce a slurry that was tape cast to yield thin green sheets of thickness $\sim 47 \mu\text{m}$. These sheets were dried at 60 °C and cut into small pieces. To form the inner electrodes [Fig. 1(b)], Pt was screen printed onto green sheets. These green sheets with the Pt inner electrodes were laminated, pressed, and cut to form the green MLC. To burn off the binder, the green

^{a)} Author to whom correspondence should be addressed. Electronic mail: h_sakyo@murata.com.

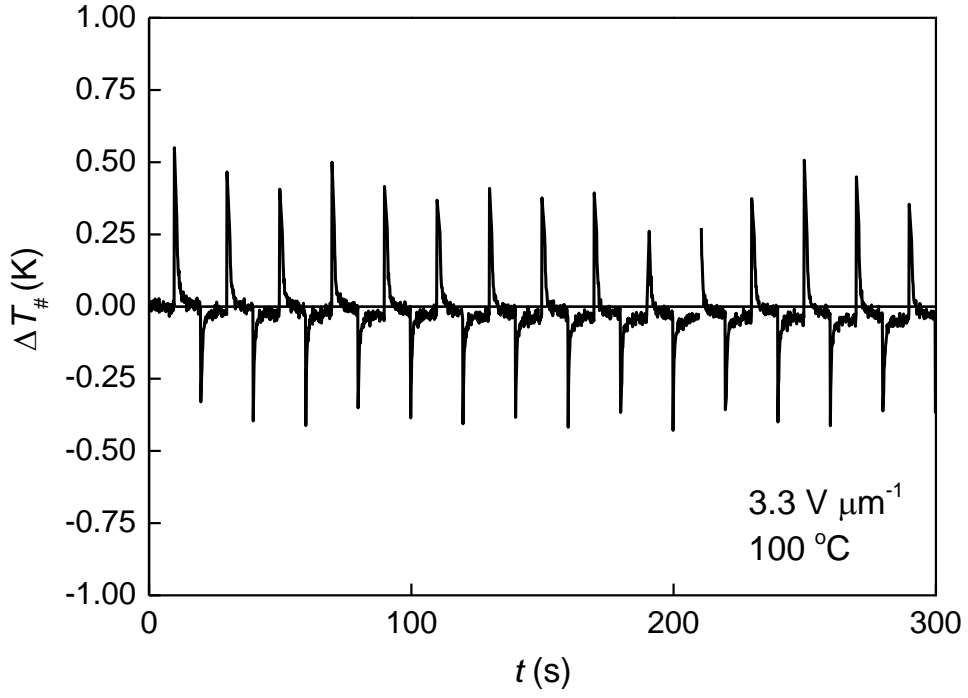
MLC was gradually heated up to 450 °C for 40 hours, kept at that temperature for 1 hour, and then cooled to room temperature. Finally, the MLC was sintered at 1150 °C for 4 hours with PbZrO₃ powder to prevent Pb deficiency. Ag outer electrodes were attached to both sides, and fired at 750 °C to connect with inner electrodes. From x-ray diffraction measurements of our plate ceramic, which was co-sintered with the MLC, we infer that our MLC should include several percent of a pyrochlore impurity phase.

Plate ceramic fabrication employed equivalent green sheets and equivalent fabrication conditions. The sintered plate ceramic measured approximately 5 mm × 5 mm × 0.3 mm. Pt electrodes of thickness 200-300 nm were deposited on both faces by RF sputtering.

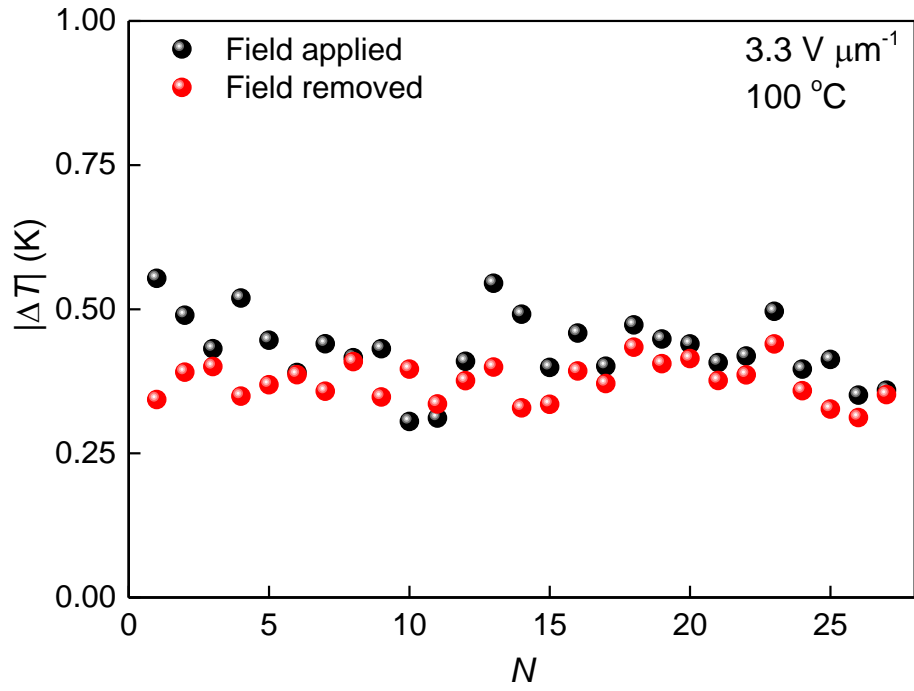
Measurement methods

Dielectric properties were measured using a broadband dielectric spectrometer (Novocontrol Technologies GmbH & Co. KG). Ferroelectric polarization was measured using a ferroelectric test system (Radiant Technologies, Inc.). Direct measurements of temperature change ΔT were performed using a sourcemeter (Advantest, R8340A) to read data from an extra-fine pointed K-type thermocouple attached to the MLC surface lying parallel to the inner electrodes, or the sputtered Pt electrode of our plate ceramic. Temperature control was achieved using a Cu block and heater, in the chamber of a manual probe station that was open to air.

Exemplary data for the ceramic plate obtained with $|\Delta E| = 3.3 \text{ V } \mu\text{m}^{-1}$ are shown in Sup. Fig. 1, overleaf. Observed variations in adiabatic temperature change $|\Delta T|$ could arise from the small volume of plate ceramic and/or the electrical noise caused by field application. By averaging over $N = 27$ jumps, we infer a value of $|\Delta T| = 0.3 \text{ K}$ for Table 1. Similar data for smaller fields were also used to construct the inset of Fig. 3(b) showing $|\Delta T|$ versus $|\Delta E|$.



(a)



(b)

Sup. Fig. 1. Plate ceramic at 100 °C. (a) Measured temperature change $\Delta T_{\#}$ versus time t due to the application and removal of $3.3 \text{ V } \mu\text{m}^{-1}$. (b) The resulting adiabatic temperature change ΔT averaged over the number of measured jumps N , from which we infer $|\Delta T| = 0.3 \text{ K}$.